

CORRECTION

View Article Online  
View Journal | View Issue



Cite this: *Ind. Chem. Mater.*, 2023, 1, 620

DOI: 10.1039/d3im90006a

rsc.li/icm

# Correction: Lithium-mediated electrochemical dinitrogen reduction reaction

Muhammad Saqlain Iqbal,<sup>b</sup> Yukun Ruan,<sup>a</sup> Ramsha Iftikhar,<sup>c</sup> Faiza Zahid Khan,<sup>d</sup> Weixiang Li,<sup>a</sup> Leiduan Hao,<sup>\*a</sup> Alex W. Robertson,<sup>e</sup> Gianluca Percoco<sup>f</sup> and Zhenyu Sun<sup>\*a</sup>

Correction for 'Lithium-mediated electrochemical dinitrogen reduction reaction' by Muhammad Saqlain Iqbal et al., *Ind. Chem. Mater.*, 2023, DOI: <https://doi.org/10.1039/D3IM00006K>.

The authors regret that the incorrect permissions were provided in the figure captions of Fig. 1–15 in the original article. The correct versions of the figures, including the updated permissions, are shown below.

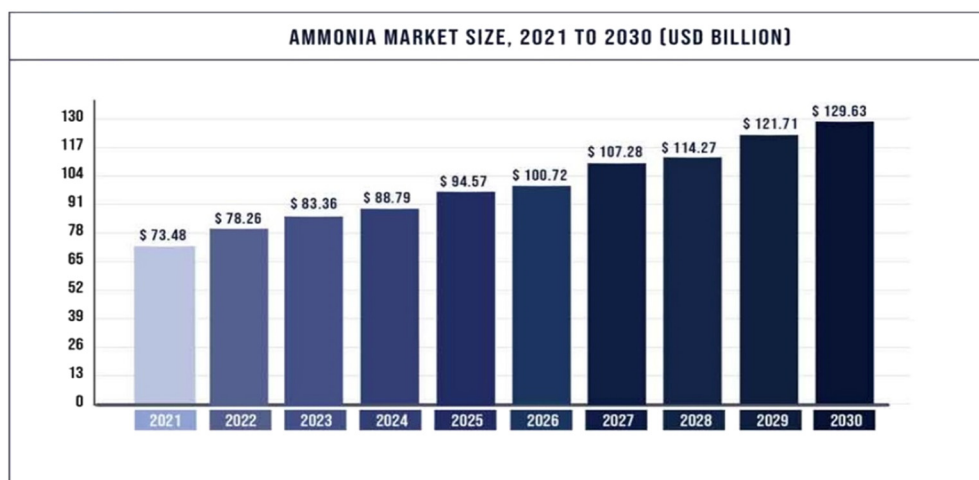


Fig. 1 Projected global ammonia demand growth from 2021 to 2030.<sup>2</sup> Copyright 2023, Precedence Research.

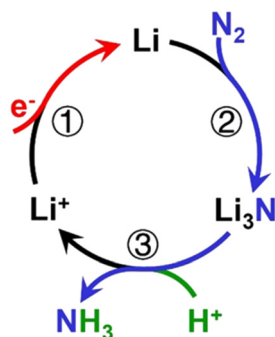


Fig. 2 Mechanism of catalytic recycling of lithium intermediates. Reproduced with permission.<sup>23</sup> Copyright 2021, Wiley-VCH.

<sup>a</sup> State Key Laboratory of Organic-Inorganic Composites, College of Chemical Engineering, Beijing University of Chemical Technology, Beijing 100029, P. R. China. E-mail: haold@buct.edu.cn, sunzy@mail.buct.edu.cn

<sup>b</sup> Department of Electrical and Information Engineering, Polytechnic University of Bari, Via E. Orabona 4, 70125 Bari, Italy

<sup>c</sup> School of Chemistry, University of New South Wales, 2033 Sydney, Australia

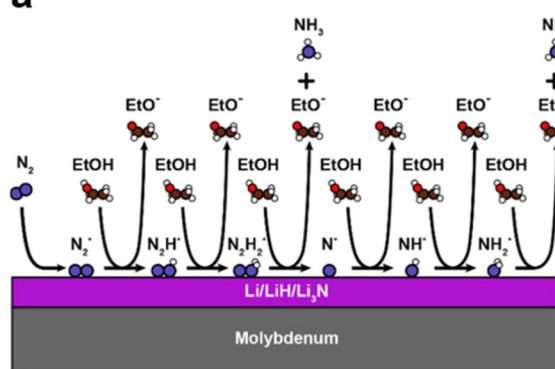
<sup>d</sup> Institute of Chemistry, Rheinische Friedrich-Wilhelms-Universität Bonn, 53113 Bonn, Germany

<sup>e</sup> Department of Physics, University of Warwick, Coventry CV4 7AL, UK

<sup>f</sup> Department of Mechanics, Mathematics and Management, Polytechnic University of Bari, Via E. Orabona 4, 70125 Bari, Italy



## a Heterogeneous Mechanism



## b

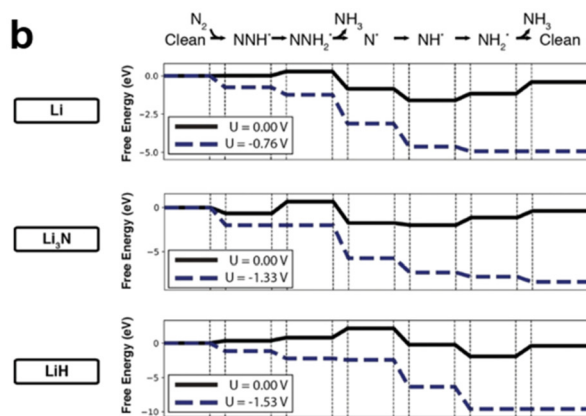


Fig. 3 (a) A 'Heterogeneous mechanism', in which there is a stable amount of lithium on the electrode at all times; (b) free energy diagram of  $\text{NH}_3$  formation on the surfaces of  $\text{Li}$ ,  $\text{Li}_3\text{N}$ , and  $\text{LiH}$ . The free energy diagram is represented through dash lines when the limiting potential is switched on. All of these surfaces are active for  $\text{NH}_3$  synthesis. Reproduced with permission.<sup>41</sup> Copyright 2020, Wiley-VCH.

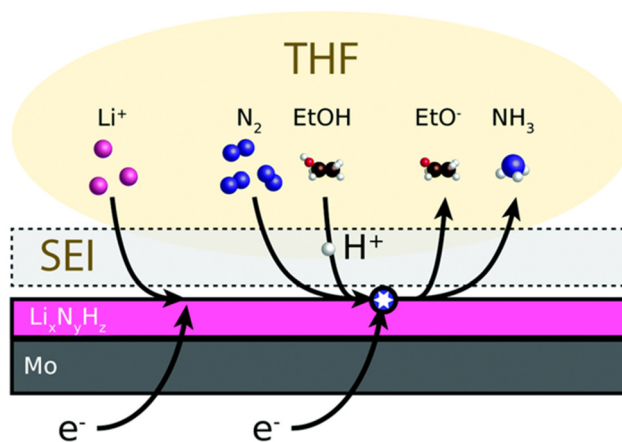


Fig. 4 Schematic of the mechanism for  $\text{Li-eN}_2\text{RR}$  to  $\text{NH}_3$ . A non-aqueous electrolyte (THF) contains lithium salt which is electrodeposited onto a metal electrode (Mo) as metallic  $\text{Li}$ . Reproduced with permission.<sup>38</sup> Copyright 2020, Royal Society of Chemistry.

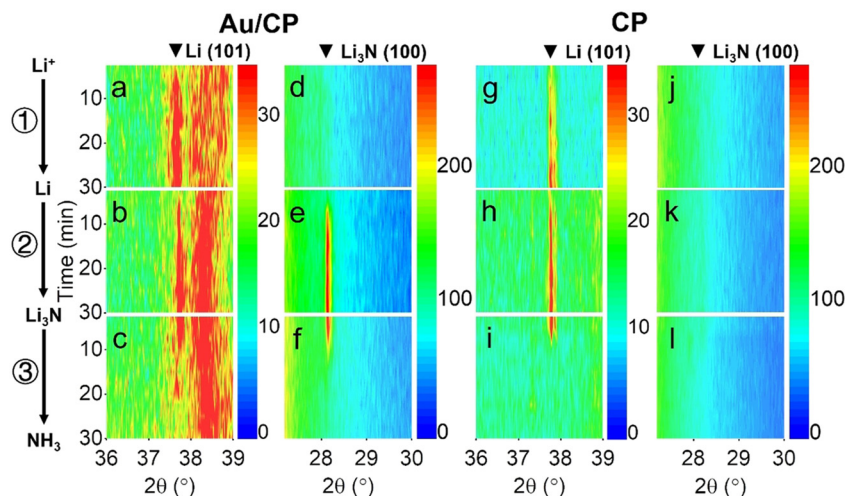


Fig. 5 *In situ* XRD contour maps of (a) and (d) Au/CP and; (g) and (j) CP under Ar atmosphere; (b) and (e) Au/CP and (h) and (k) CP under  $\text{N}_2$  atmosphere without EtOH; (c) and (f) Au/CP and (i) and (l) CP under  $\text{N}_2$  atmosphere with EtOH. Reproduced with permission.<sup>23</sup> Copyright 2021, Wiley-VCH.

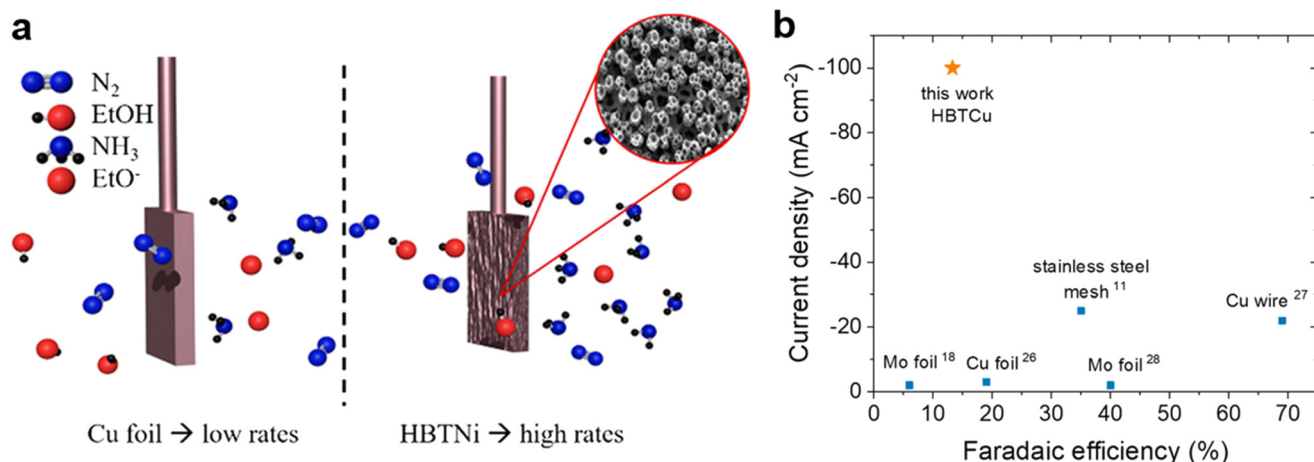


Fig. 6 (a) Illustration of Cu foil and HBT Cu for Li-mediated  $eN_2RR$ ; (b) comparison of HBT Cu and previously reported electrode materials in terms of current density and  $NH_3$  FE. Reproduced with permission.<sup>58</sup> Copyright 2022, American Chemical Society.

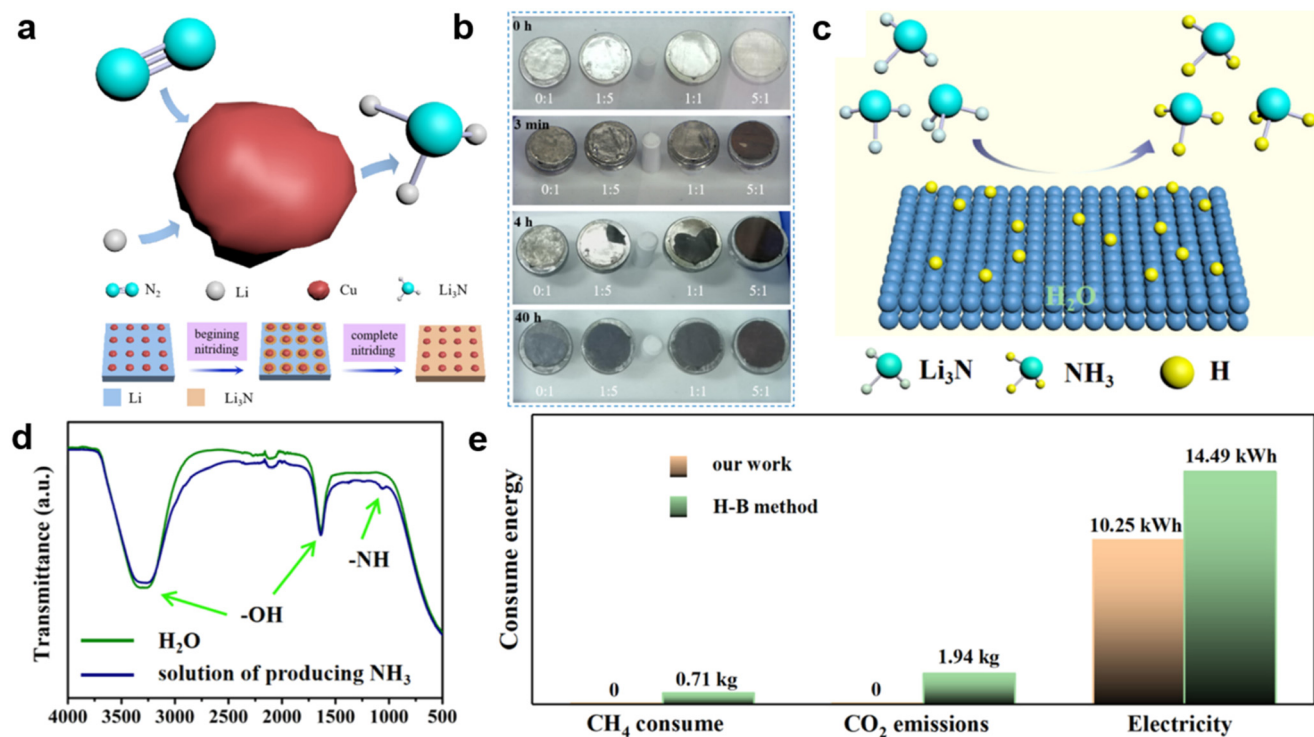
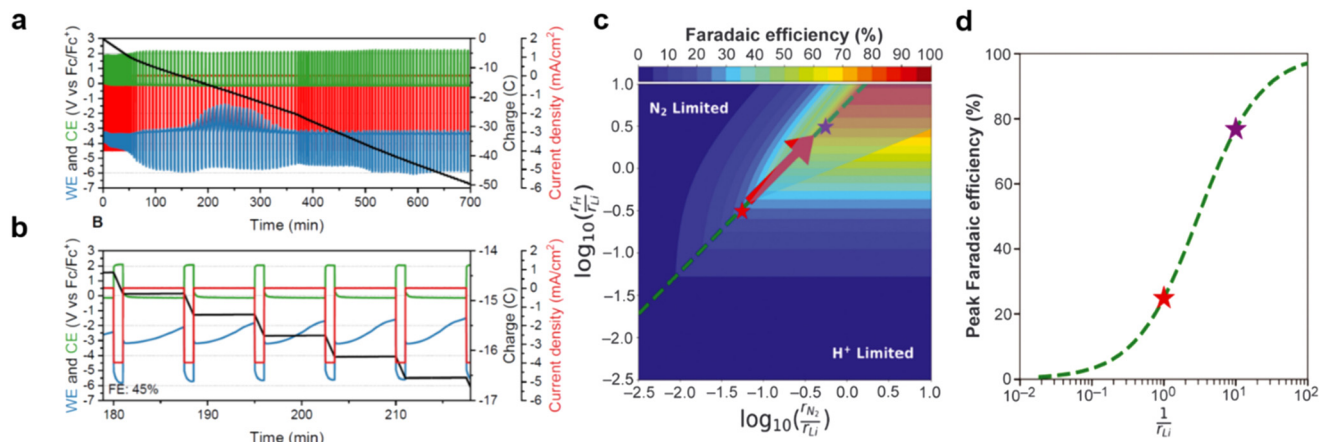
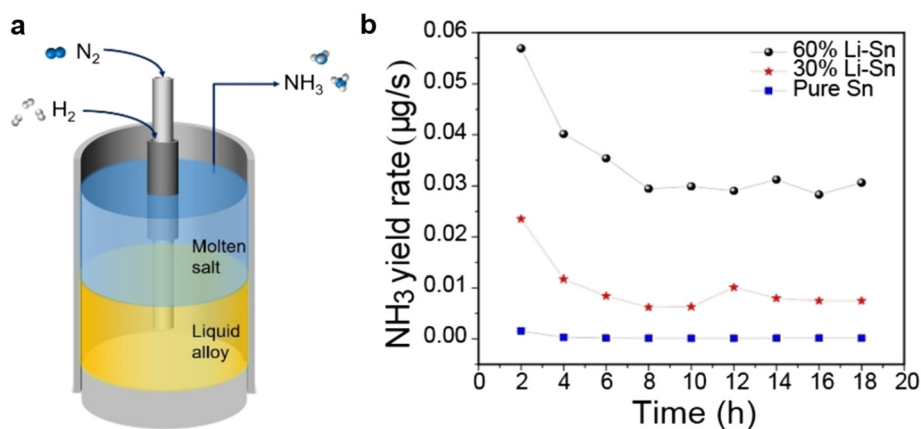


Fig. 7 (a) Illustration of Cu-catalyzed lithium nitridation (top panel) and steps for the formation of  $Li_3N/Cu$  from  $Li/Cu$  (bottom panel); (b) catalytic effect of Cu-to-Li mass ratio on the nitridation process; (c) illustration of  $NH_3$  synthesis from the reaction of  $Li_3N$  and  $H_2O$ ; (d) infrared spectra of  $H_2O$  and the electrolyte solution after reaction; (e) comparison of this work with the H-B process in terms of energy consumption for production of 1 kg of  $NH_3$ . Reproduced with permission.<sup>14</sup> Copyright 2022, American Chemical Society.





**Fig. 8** (a) Cycling method between  $-2.0$  and  $0.0 \text{ mA cm}^{-2}$  (red) for a total of  $100 \text{ C}$  of charge passed (black); (b) a close-up of the cycling; reproduced with permission.<sup>38</sup> Copyright 2020, Royal Society of Chemistry; (c) heatmap of the predicted FE against the ratio of  $\text{N}_2$  to lithium (x axis) and proton to lithium (y axis) diffusion rates; (d) a one-dimensional plot of  $\text{NH}_3$  FE cut along the optimal  $r_{\text{N}_2}/r_{\text{H}}$  ratio. Reproduced with permission.<sup>59</sup> Copyright 2021, American Association for the Advancement of Science.



**Fig. 9** (a) Graphical illustration of Li-eN<sub>2</sub>RR containing Li-Sn alloy and molten LiCl-KCl salt forming a biphasic system; (b)  $\text{NH}_3$  yield rate against electrolysis time on Li-Sn and pure Sn. Reproduced with permission.<sup>62</sup> Copyright 2021, Wiley-VCH.

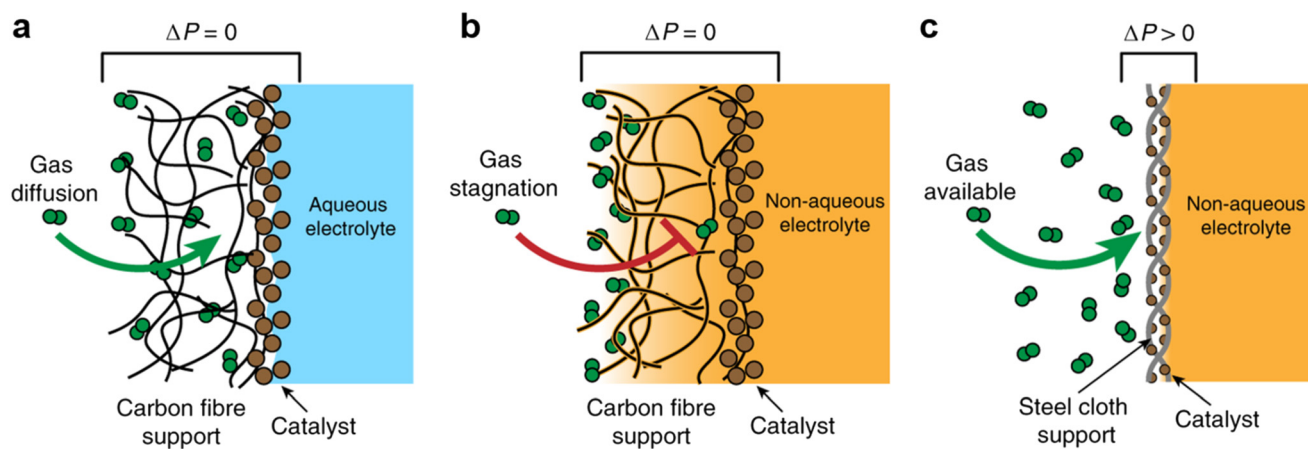


**Fig. 10** (a) A hydrophobic GDE with an aqueous electrolyte; (b) a hydrophobic GDE with a non-aqueous electrolyte; (c) a catalyst-coated (SSC) GDE with a non-aqueous electrolyte. Reproduced with permission.<sup>22</sup> Copyright 2020, Springer Nature.





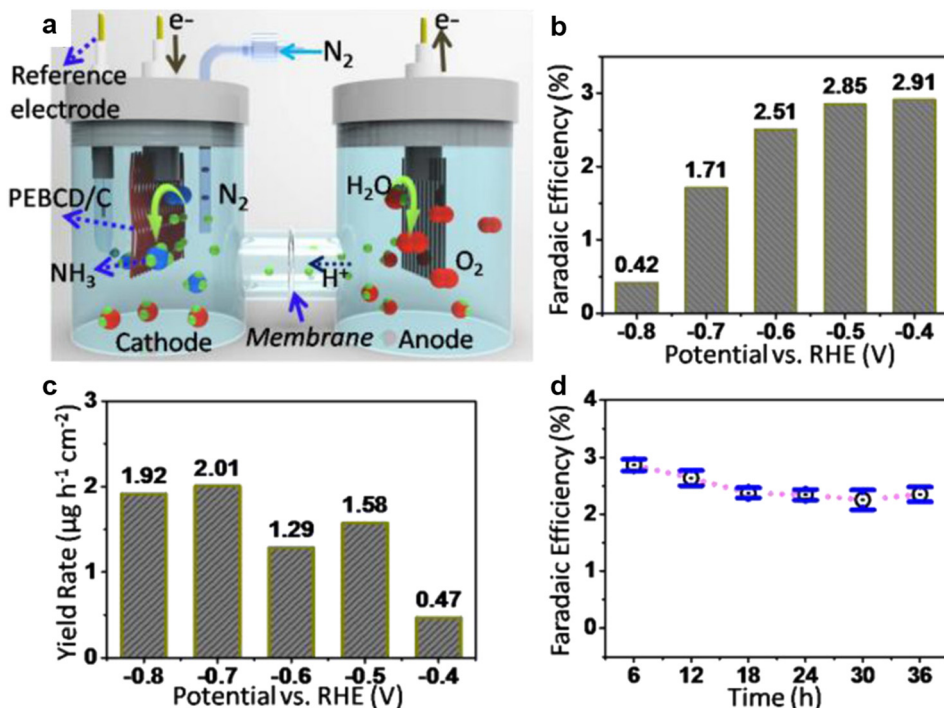


Fig. 11 (a) The graphic illustration of the configuration of the electrochemical cell for the eN<sub>2</sub>RR process; (b) FEs of the Li<sup>+</sup>-PEBCD/CC catalyst at different potentials during the eN<sub>2</sub>RR; (c) NH<sub>3</sub> yield rate against applied potential during the eN<sub>2</sub>RR; (d) durability test results for Li<sup>+</sup>-PEBCD/CC. Reproduced with permission.<sup>3</sup> Copyright 2017, American Chemical Society.

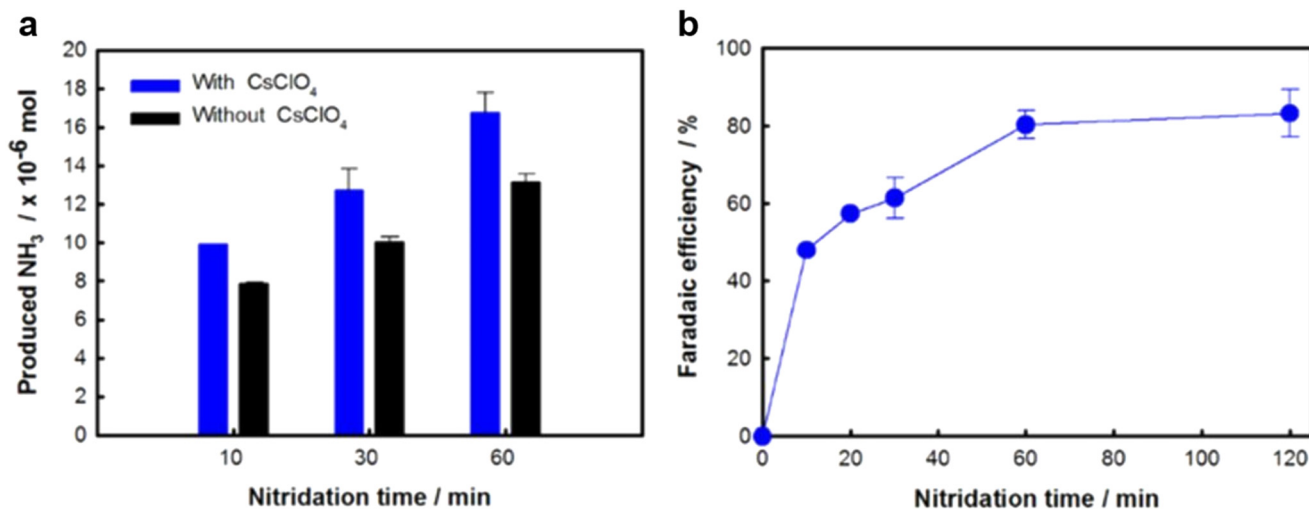


Fig. 12 (a) NH<sub>3</sub> yield and (b) NH<sub>3</sub> FE in the presence and absence of 0.03 M CsClO<sub>4</sub> at 220 °C over time. Reproduced with permission.<sup>8</sup> Copyright 2018, IOP Publishing.



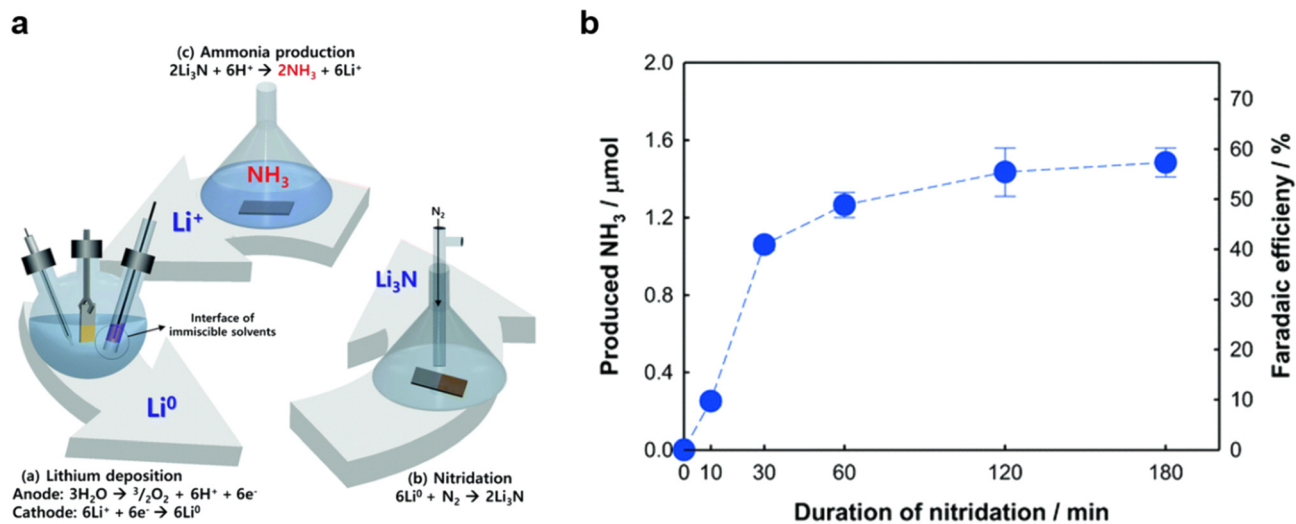


Fig. 13 (a) Schematic diagram and (b)  $\text{NH}_3$  yield and FE of the biphasic hybrid catalytic system catalyzed by  $\text{LiClO}_4$  (aq) and  $\text{LiClO}_4$ -PMMA composite. Reproduced with permission.<sup>66</sup> Copyright 2019, Royal Society of Chemistry.

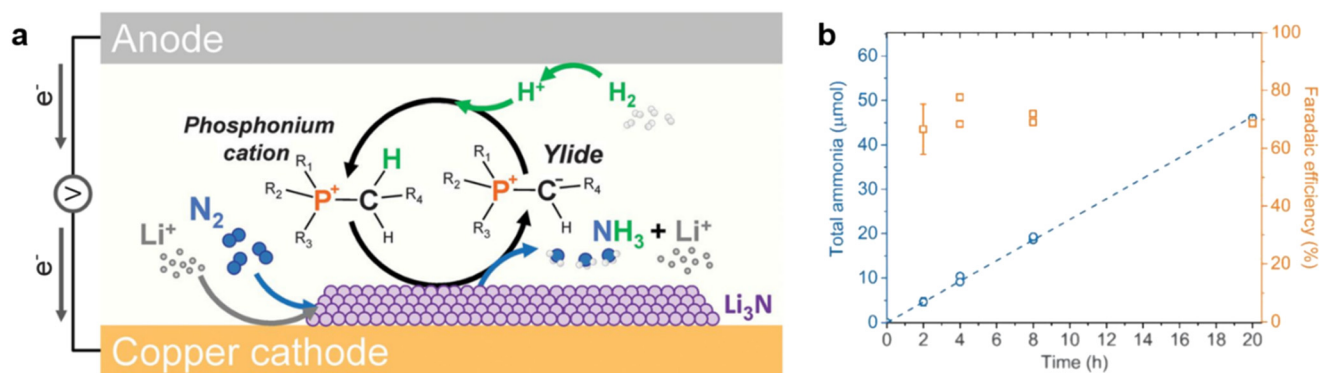


Fig. 14 (a) Schematic illustration of  $\text{eN}_2\text{RR}$  catalysis using a phosphonium salt; (b)  $\text{NH}_3$  yield and FE as a function of time. Reproduced with permission.<sup>24</sup> Copyright 2021, American Association for the Advancement of Science.

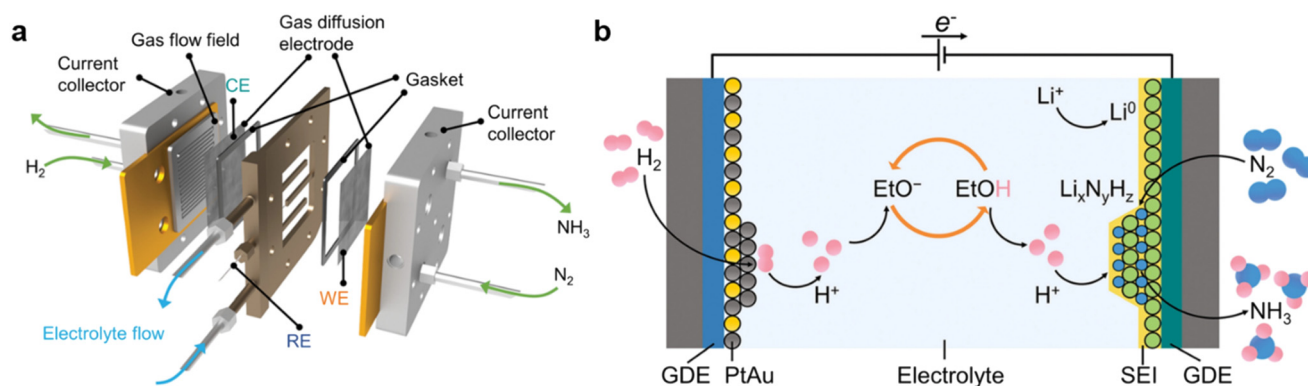


Fig. 15 (a) Expanded view of the continuous-flow electrolyzer configuration; (b) schematic process of the Li-NRR in a continuous-flow electrolyzer. Reproduced with permission.<sup>72</sup> Copyright 2023, American Association for the Advancement of Science.

The Royal Society of Chemistry apologises for these errors and any consequent inconvenience to authors and readers.

